Laser Flash-Induced Kinetic Analysis of Cytochrome *f* Oxidation by Wild-Type and Mutant Plastocyanin from the Cyanobacterium *Nostoc* sp. PCC 7119[†]

Cristina Albarrán, José A. Navarro, Fernando P. Molina-Heredia, Piedad del S. Murdoch, Miguel A. De la Rosa, and Manuel Hervás*

Instituto de Bioquímica Vegetal y Fotosíntesis, Centro de Investigaciones Científicas Isla de la Cartuja, Universidad de Sevilla y Consejo Superior de Investigaciones Científicas, Sevilla, Spain

ABSTRACT: Oxidation of the soluble, truncated form of cytochrome *f* by wild-type and mutant species of plastocyanin has been analyzed by laser flash absorption spectroscopy in the cyanobacterium *Nostoc* (formerly, *Anabaena*) sp. PCC 7119. At low ionic strengths, the apparent electron transfer rate constant of cytochrome *f* oxidation by wild-type plastocyanin is 1.34×10^4 s^{-1}, a value much larger than those determined for the same proteins from other organisms. Upon site-directed mutagenesis of specific residues at the plastocyanin interaction area, the rate constant decreases in all cases yet to varying extents. The only exception is the D54K variant, which exhibits a higher reactivity toward cytochrome *f*. In most cases, the reaction rate constant decreases monotonically with an increase in ionic strength. The observed changes in the reaction mechanism and rate constants are in agreement with the location of the mutated residues at the interface area, as well as with the peculiar orientation of the two partners within the *Nostoc* plastocyanin−cytochrome *f* transient complex, whose NMR structure has been determined recently. Furthermore, the experimental data herein reported match well the kinetic behavior exhibited by the same set of plastocyanin mutants when acting as donors of electrons to photosystem I [Molina-Heredia, F. P., et al. (2001) *J. Biol. Chem. 276*, 601−605], thus indicating that the copper protein uses the same surface areas—one hydrophobic and the other electrostatic—to interact with both cytochrome *f* and photosystem I.

Cytochrome (Cyt)[1] *f* (33 kDa), a *c*-type Cyt, is one of the four integral redox components of the Cyt b_6f complex of the thylakoidal membrane in oxygenic photosynthetic organisms, where it accepts electrons from the Rieske iron−sulfur protein and passes them to P_{700}^+ in photosystem I (PSI) via the luminal electron carriers plastocyanin (Pc) and Cyt c_6 (*1, 2*). Cyt *f* has been purified from a variety of plant, algal, and cyanobacterial sources, and its overall three-dimensional structure has shown to be highly conserved (*3−7*). However, the surface electrostatic potential of Cyt *f* varies considerably from one organism to another, the protein being highly positive in eukaryotes but slightly negative in cyanobacteria (*1, 3*). In fact, a conserved basic ridge is present in plant and algal Cyt *f*, but is replaced with more diffusely arranged acidic residues in cyanobacterial proteins. Because of the low water solubility of native Cyt *f*, the soluble truncated forms of the protein from different sources have been used with great success to perform both structural and functional in vitro studies (*6−13*).

Extensive kinetic and structural analyses of the transient Pc−Cyt *f* complex have been carried out in an ample variety of organisms, with relevant differences being observed with regard to the reaction mechanism and relative orientation of the two partners inside the complex (*8, 9*). First, the redox interaction is mainly hydrophobic in the cyanobacterium *Phormidium laminosum* (*8, 9*) but electrostatically driven in plants. Second, Pc binds to Cyt *f* in a "head-on" conformation in *Phormidium*, in which the hydrophobic patch of Pc (the so-called site 1) accounts for the whole recognition interface area, but in a "side-on" orientation in plants, with the acidic patch of Pc (so-called site 2) being involved as well (see ref *9* for a recent review).

Pc and Cyt *f* from the cyanobacterium *Nostoc* sp. PCC 7119, in particular, form a highly interesting system as they react with each other by means of attractive electrostatic interactions, like plant proteins, but using differently charged patches, which are positive in Pc and negative in Cyt *f*. Noteworthy is the fact that the three-dimensional structure of the *Nostoc* Pc−Cyt *f* complex has been recently characterized by NMR spectroscopy (*14*), thus revealing significant differences regarding the relative orientation of both proteins within the complex as compared with that previously reported for plants and *Phormidium*. Actually, the conformation of the *Nostoc* Pc−Cyt *f* complex resembles the characteristic

---

* To whom correspondence should be addressed: Instituto de Bioquímica Vegetal y Fotosíntesis, Universidad de Sevilla y CSIC, Américo Vespucio 49, 41092 Sevilla, Spain. Telephone: 34-954-489-514. Fax: 34-954-460-065. E-mail: mhervas@us.es.

[1] Abbreviations: Cyt, cytochrome; dRf, deazariboflavin; k_2, second-order rate constant; K_A, equilibrium constant for complex formation; k'_{et}, apparent electron transfer rate constant; k_{obs}, observed pseudo-first-order rate constant; Pc, plastocyanin; PDQ, propylendiquat; PSI, photosystem I; WT, wild-type.

side-on binding mode present in plants, although with an interface similar to that of the *Phormidium* complex.

Here we report a laser flash-induced kinetic analysis of Cyt *f* oxidation by the wild-type species and site-directed mutants of Pc, thus providing novel insights into the peculiar structural features of the *Nostoc* Pc−Cyt *f* complex. Every Pc variant herein used contains just one modified residue at the interaction area, whereas Cyt *f* is the soluble, recombinant fragment resulting from overexpression in *Escherichia coli* cells of a truncated *pet*A gene at which the nucleotide region encoding the 35-amino acid hydrophobic tail has been removed. The kinetic efficiencies of Pc mutants in oxidizing Cyt *f* are indeed compared with their respective efficiencies in donating electrons to PSI, which have been previously determined (see ref *15* for a review).

EXPERIMENTAL PROCEDURES

Cloning of the petA Gene. The direct primer TTG CCC CTA TAG AGA TGA GAA AT and the reverse one TTA AAA GTA TTG ATT TAT CAG AGA designed from the known sequence of *pet*A, encoding Cyt *f* in *Nostoc* sp. PCC 7120 (*16*), were used to amplify the region containing the *pet*A gene from the genomic DNA of *Nostoc* sp. PCC 7119 by the polymerase chain reaction (PCR). The resulting *pet*A gene was sequenced[2] and cloned using the pGEM-T cloning kit (Promega).

To replace the Cyt *f* leader sequence with that of Cyt c_6 and truncate the region encoding the hydrophobic tail of the protein, a second PCR step was designed by using the adaptamer technology (*17, 18*); both the plasmid containing the *pet*A gene and the expression plasmid for the *pet*J gene were used as the template (*19*). The direct primer TCT CAA GGA TCC TTA TTT GCA GAG A was designed from the nucleotide sequence encoding for the transit peptide of Cyt c_6 from *Nostoc*, introducing a BamHI restriction site upstream of the 5′ end of the leader of this primer to facilitate cloning of the generated PCR product. The reverse primer GCA ATC AAC CCA GCC AAC TCT ATT AGC ATC TT was designed from the *pet*A nucleotide sequence, introducing a stop codon after Asn-252 to remove the hydrophobic tail. The adaptamers are chimerical oligonucleotides complementary to two different DNA sequences. Two adaptamers were designed with their sequences (CTT CAG TAG CCC TGC ATT AGC ATA CCT TTC TGG GCG CAG CA and TGC TGC GCC CAG AAA GGA TAT GCT AAT GCA GGG CTA CTG AAG) overlapping the sequences of the leader of Cyt c_6 and truncated Cyt *f*. The adaptamers were added to the PCR mixture in a 1/100 ratio with respect to the previous one. Thus, in a single PCR step (*17*), a chimeric *pet*A gene that encodes Cyt *f* without the hydrophobic C-terminus and with the Cyt c_6 transit peptide from *Nostoc* was obtained. The chimeric gene was sequenced and cloned as described previously, and the commercial plasmid pBluescript II SK(+) (Stratagene) was used to obtain the pEAF-wt expression vector. *E. coli* strain DH5α (Bethesda Research Laboratories, Bethesda, MD) was used for cloning, plasmid construction, and expression of the cloned gene. Other molecular biology protocols were standard.

Purification of Native Cytochrome f and Expression and Purification of the Recombinant Protein. *Nostoc* sp. PCC 7119 was grown in standard BG11 medium (*20*). Native *Nostoc* Cyt *f* was isolated from thylakoidal fragments by ethyl acetate extraction (*21, 22*). After extraction, the sample was dialyzed against 2 mM Tris-HCl (pH 8.0), 5% glycerol, and 0.02% Triton X-100. Further purification was carried out by two consecutive ion-exchange chromatographies (DEAE-cellulose, elution gradient from 0 to 0.4 M NaCl in the same buffer). The fractions containing Cyt *f* were desalted, and the buffer was replaced with 150 mM NaCl in 50 mM phosphate buffer (pH 8.0). After concentration by ultrafiltration (Amicon, 10 kDa cutoff), Cyt *f* samples were purified by FPLC in a gel filtration column (Pharmacia HiLoad 16/60 Superdex 75). Protein concentrations were determined spectrophotometrically using an absorption coefficient of 31.5 mM^{-1} cm^{-1} at 556 nm previously described for reduced turnip Cyt *f* (*23*). An A_{275}/A_{556} ratio of 2.75 was obtained at the end of the partial purification process.

To improve the maturation and correct insertion of the heme group, *E. coli* DH5α cells cotransformed with plasmids pEAF-wt and pEC86 (*24*) were used for expression of the cloned gene. The cells were grown for 24 h at 100 rpm and 37 °C in 2 L (in 5 L Erlenmeyer flasks) of standard Luria-Bertani (LB) medium (*25*) supplemented with 6 μg/L Fe-$(NH_4)_3$ citrate, 100 μg/mL ampicilline, and 12 μg/mL chloramphenicol.

The cell periplasmic fraction was extracted by freeze−thaw cycles (*26*). Solid ammonium sulfate was added to the periplasmic suspension up to 40% saturation. After centrifugation, ammonium sulfate was added to the resulting supernatant up to 70% saturation. The final pellet was resuspended in 5 mM Tris-HCl buffer (pH 8.0), extensively dialyzed against the same buffer, and applied to a DEAE-cellulose column equilibrated with the same buffer. Cyt *f* was eluted with a 0 to 0.5 M NaCl gradient in 5 mM Tris-HCl (pH 8.0). The fractions containing Cyt *f* were pooled, dialyzed against 5 mM MES (pH 6.0), concentrated, and purified by FPLC using an ion-exchange column (UNO Q-6, Bio-Rad). The recombinant protein was eluted with a 0 to 0.5 M NaCl gradient in 5 mM MES (pH 6.0). Cyt *f* fractions were dialyzed against 5 mM Tris-acetate (pH 8.0), applied to a chromatofocusing column, and eluted with Polybuffer Exchanger 74 (Sigma). An A_{275}/A_{556} ratio of 1.2 was obtained for pure protein in its reduced state.

Nostoc WT Pc and its mutants were expressed and purified as described previously (*19, 27*).

Analytical Methods. The molecular mass, isoelectric point, and redox potential of native and recombinant Cyt *f* were determined as previously described (*19*), except that the absorbance changes were monitored at 556 minus 580 nm. The N-terminal amino acid sequences were determined in a Procise TM 494 protein sequencer (Applied Biosystems). The extinction coefficient of reduced Cyt *f* at 556.5 nm was calculated using the method described in ref *28*.

Laser Flash Absorption Spectroscopy. Laser flash experiments were performed anaerobically at room temperature in a 1 cm path length cuvette as previously described (*29*). In the absence of protein, the laser flash generates 5-deazariboflavin (dRf) radicals (dRfH•), which rapidly (<1 μs) reduce propylendiquat (PDQ), a positively charged viologen analogue, to its reduced species (PDQ•+) (*30*). In the presence

---

[2] The EMBL accession number for the *Nostoc* sp. PCC 7119 *pet*A gene is AJ749608.

of oxidized proteins, PDQ$^{\bullet+}$ reduces Cyt *f*, which is in excess over Pc, and the heme protein in turn reduces Pc.

The redox changes of PDQ, Cyt *f*, and Pc were monitored at 510, 556, and 597 nm, respectively. The standard reaction mixture contained, in a final volume of 1 mL, 5 mM sodium phosphate (pH 7.0), 2.5 mM EDTA, 2 mM PDQ, 100 μM dRf, 50 μM Cyt *f*, and Pc at varying concentrations. Small volumes of a concentrated solution of sodium chloride were added to adjust the ionic strength. Protein concentrations were determined using the following absorption coefficients: $\epsilon_{556} = 31.8$ mM^{-1} cm^{-1} (this work) and $\epsilon_{597} = 4.5$ mM^{-1} cm^{-1} (*19*) for reduced Cyt *f* and oxidized Pc, respectively. All experiments were performed under pseudo-first-order conditions, for which the amount of acceptor protein (oxidized Pc) was maintained well in excess over the amount of reduced Cyt *f*. Each kinetic trace was the average of 8−12 measurements, with a 30 s time spacing between flashes. Kinetic analyses were performed according to the reaction mechanisms previously proposed (*31*).

RESULTS AND DISCUSSION

On the basis of the known sequence of the *pet*A gene from *Nostoc* sp. PCC 7120 (*16*), a couple of oligonucleotides were designed to amplify and clone the complete gene *pet*A from *Nostoc* sp. PCC 7119. In a second PCR step, the native transit peptide of Cyt *f* was replaced with a more typical bacterial leader sequence, the transit peptide of Cyt c_6 from *Nostoc*, which has been shown to significantly enhance the final yield of other recombinant *c*-type Cyts in *E. coli* (*17*, *19*, *32*), and the region encoding the hydrophobic tail was truncated. A DNA band of 860 bp was obtained in this second PCR amplification step (not shown), with the sequence encoding Cyt *f* being truncated after Asn-252 to remove the 35-amino acid C-terminal transmembrane anchor, and with the Cyt c_6 transit peptide. This band was recovered and ligated using the pGEM-T cloning kit. ApaI and BamHI were used as the cloning sites in pBluescript SK(+) to obtain the pEAF-wt expression plasmid.

After several *E. coli* strains had been checked for the production of recombinant Cyt *f*, the highest protein yield was obtained with *E. coli* DH5α cotransformed with plasmids pEAF-wt and pEC86. The final yield of protein from the periplasmic fraction was 1.5 mg/L of culture. This figure varies considerably depending on the oxygen content of the medium, with the best results obtained by stirring the culture at 100 rpm. The recombinant protein can thus be purified with losses of less than 30% due to the absence of the hydrophobic tail, milligram quantities of protein being obtained in a few days.

The UV−vis electronic absorption spectra of the truncated recombinant Cyt *f* in its reduced and oxidized forms are identical to those of the native protein, with the same absorbance maxima of the α, β, and γ bands of the reduced form. *Nostoc* Cyt *f* shows a maximum at 556.5 nm for the α band of the reduced form, typical of other cyanobacterial Cyt *f* α bands (*33*), whereas eukaryotic Cyt *f* presents an α band with a maximum at 554 nm. The calculated extinction coefficients are similar for native and recombinant proteins, and in agreement with that described for turnip Cyt *f* (31.5 mM^{-1} cm^{-1}) (*23*). Other physicochemical properties of the recombinant protein were practically identical to those of
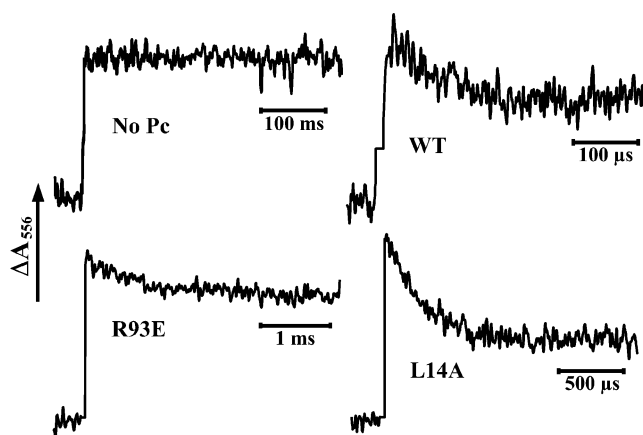

FIGURE 1: Kinetic traces showing fast reduction of cytochrome *f* by PDQ$^{\bullet+}$, and oxidation of the heme protein by WT and mutant species of plastocyanin. Cytochrome *f* and plastocyanin were at final concentrations of 50 and 20 μM, respectively. In all cases, the kinetic traces were fitted to single-exponential curves. Other conditions were as described in Experimental Procedures.

the native protein purified from *Nostoc* cells, including the midpoint redox potential value ($E'_m = 334 \pm 4$ mV at pH 7.0), which is similar to those previously described for Cyt *f* from other sources and is pH-independent within the pH range of 5−9 (not shown). The recombinant protein was properly expressed and matured in *E. coli*, as deduced from the identical N-terminal amino acid sequence compared with that of the *Nostoc* native protein (not shown). This is an important feature as Tyr-1 is one of the Fe heme ligands (*6*). In summary, the high degree of similarity of the analyzed physicochemical properties of truncated and native Cyt *f* validates the use of the recombinant heme protein for the functional study herein reported.

The use of dRf ($E'_m = -0.65$ V) in combination with a positively charged probe, such as the viologen analogue radical PDQ$^{\bullet+}$ ($E'_m = -0.55$ V), allows us to study electron transfer between redox proteins where it is necessary to force the preferential reactivity toward redox centers located in a negative electrostatic area (*30*, *34*, *35*), as the negative Cyt *f* from *Nostoc*.

The individual electron transfer reactions from PDQ$^{\bullet+}$ to either oxidized Cyt *f* (Figure 1, upper left) or Pc (not shown) were analyzed. The corresponding pseudo-first-order observed rate constant (k_{obs}) depends linearly on protein concentration (not shown), and from the slope of this plot, second-order rate constants (k_2) of 4.8×10^9 M^{-1} s^{-1} for Cyt *f* and 4.6×10^8 M^{-1} s^{-1} for Pc reduction were determined. PDQ$^{\bullet+}$ donates electrons to Cyt *f* 10 times more efficiently than it reduces Pc. This preference in reactivity for the heme protein makes this method an adequate tool for analyzing the further electron transfer from Cyt *f* to Pc, with a dead time on the microsecond time scale (Figure 1). The reactivity of Pc mutants with PDQ$^{\bullet+}$ does not differ significantly from that of WT (not shown).

In the absence of Pc, reduced Cyt *f* remains stable for hundreds of milliseconds (Figure 1, top left). When Pc is added to the reaction cell containing Cyt *f* (Figure 1, WT trace), the laser-induced absorbance changes fit well with the first, fast reduction of Cyt *f* followed by the oxidation of the heme protein on a longer time scale. In fact, the slower decrease in absorbance at 556 nm does not reach the preflash baseline, thus indicating that Cyt *f* reoxidation
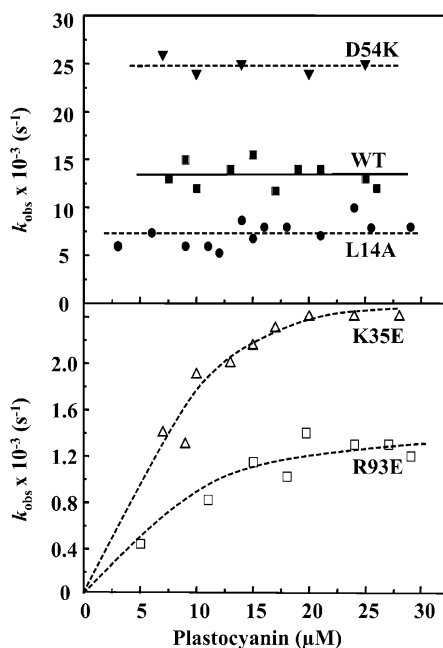
FIGURE 2: Dependence upon plastocyanin concentration of k_{obs} for cytochrome f oxidation by WT and mutant species of the copper protein. The dashed lines for mutants K35E and R93E correspond to the theoretical fitting using the formalism described in ref *11*. Experimental conditions are described in Experimental Procedures.

Scheme 1: Reaction Mechanism for the Reduction of Plastocyanin by Cytochrome f
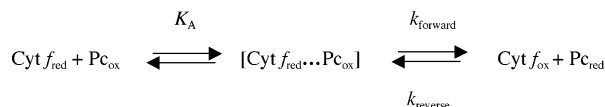
is not complete (Figure 1, WT trace). This Cyt oxidation is concomitant with the electron transfer to Pc, as inferred from the absorbance decrease at 597 nm on the same time scale (not shown). The relatively small extent of Cyt f oxidation can be explained by the similarity of the redox potentials of the two proteins, which allows a reversible electron transfer reaction up to the equilibrium (Scheme 1) (*11*). This also explains the difficulty in obtaining data points at low Pc concentrations (<5 μM), where the extent of Cyt f oxidation is very low. The k_{obs} values for Cyt f oxidation by Pc are independent of Pc concentration within the range that was analyzed (Figure 2, top), indicating that the system has a very high association constant ($K_A \geq 10^6$ M^{-1}) and allowing the estimation of an apparent first-order intracomplex electron transfer rate constant (k'_{et}). Our present estimation of K_A is sensibly higher than that previously calculated by NMR for the same system (*14*), a difference than can be ascribed to the very different experimental conditions (pH, ionic strength, redox state of the proteins, etc.) used in both cases. In this respect, it is important to bear in mind the dramatic dependence of this reaction on ionic strength (see below). The k'_{et} value of 13 400 s^{-1} calculated from these experiments (Table 1) reveals the high efficiency of the *Nostoc* system compared with the sensibly lower values of ca. 3000 s^{-1} described for electron transfer rates in eukaryotic systems (*11, 36*). The low signal-to-noise ratio ascribed to the low extent of oxidation of Cyt f (see above) prevented a reliable estimation of the forward (Cyt $f \rightarrow$ Pc) and reverse (Pc $\rightarrow$ Cyt f) electron transfer rates from the kinetic amplitudes. The estimated k'_{et} thus corresponds to a minimal value for

Table 1: Kinetic Constants for the Interaction of WT and Mutant Plastocyanin with Cytochrome f and Photosystem I

plastocyanin	ΔE (mV) (WT − mutant)	k'_{et} ($\times 10^{-3}$ s^{-1}) with Cyt f	k_2 ($\times 10^{-7}$ M^{-1} s^{-1}) with PSI[a]
WT	0	13.4	7.68
L14A	−16	7.3	1.37
K35A	5	5.2	2.55
K35E	25	3.8[b]	1.35
D54K	2	25.5	9.73
K62A	9	7.0	3.03
K62E	16	2.3	1.59
Y88A	15	13.0	4.44
Y88F	12	13.4	4.73
R93Q	19	4.5	0.99
R93E	30	1.8[b]	0.32

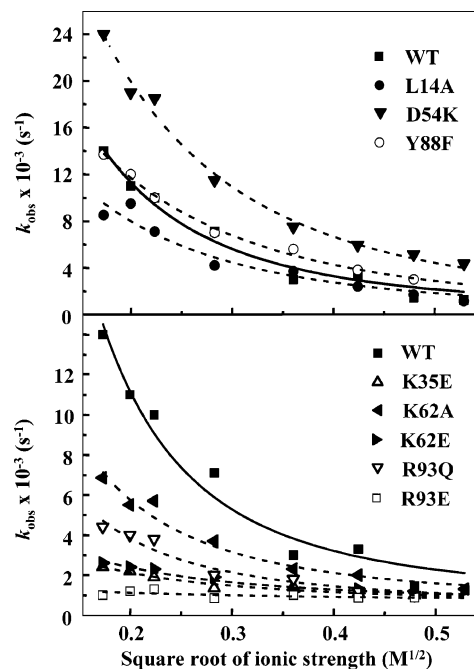[a] Data from ref *27*. [b] Minimal values estimated using the formalism of Meyer et al. (*11*).

FIGURE 3: Ionic strength dependence of k_{obs} for cytochrome f oxidation by WT and mutant species of plastocyanin. The plastocyanin concentration was 24 μM. The solid and dashed lines are for the fitting of experimental data to the equation by Watkins et al. (*37*), except for mutant R93E. Other conditions are described in Experimental Procedures.

the forward electron transfer constant. A behavior similar to that described at pH 7 is observed at the more physiological pH value of 5 (not shown). To the best of our knowledge, this is the first measurement of the apparent intracomplex rate constant for the Cyt f−Pc system in cyanobacteria.

   To analyze the nature of the Cyt f−Pc complex, the effect of ionic strength on the reaction was investigated. As can be seen in Figure 3, the k_{obs} values decreased monotonically with an increase in salt concentration up to 10^3 s^{-1} at an ionic strength of 250 mM. This behavior indicates the existence of a strong electrostatic attraction between the reactants. However, the inconvenience of increasing the ionic strength over 0.25 M because of the slow Cyt f reduction by PDQ$^{\bullet+}$ impedes a reliable determination of the rate constant at infinite ionic strength. A similar but much less pronounced ionic strength dependence has been described for the Cyt f−Pc interaction in *P. laminosum* (*10, 13*). This behavior is
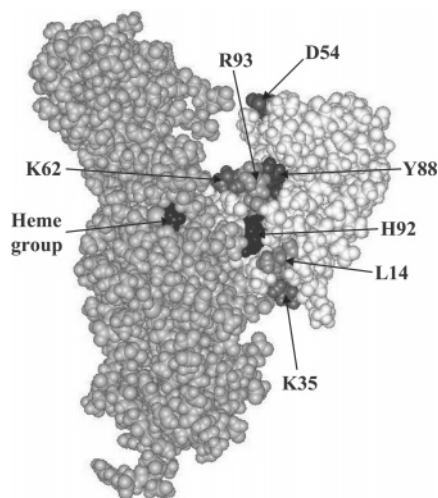
FIGURE 4: Space-filling model of the cytochrome *f*−plastocyanin complex from *Nostoc* sp. PCC 7119 showing the residues of the copper protein modified by site-directed mutagenesis. Cytochrome *f* is colored gray, whereas plastocyanin is depicted in light gray. The heme group of cytochrome *f* and the copper ligand His-92 of plastocyanin are also shown.

different from that observed in eukaryotic systems, where the dependence of the rate constant on ionic strength shows a bell-shaped profile, with an optimum value at an ionic strength of ca. 50 mM (*11*).

To establish whether Pc uses the same surface areas to interact with its two redox membrane partners, the reactivity toward Cyt *f* of a set of Pc mutants previously analyzed with PSI (*27*) was investigated here. These Pc mutants concern specific residues at the positively charged east face (D54K, K62A, K62E, Y88A, and Y88F) and at the north hydrophobic pole (L14A, K35A, and K35E), which has been shown to be involved in complex formation with Cyt *f* (Figure 4, and see ref *14*), as well as the only arginine residue (R93E and R93Q), which is adjacent to the copper site and essential for the interaction with PSI (*27*).

The kinetic profile of reduction of Pc by Cyt *f* under standard conditions was monoexponential with all mutants, as was the case for WT, but the kinetic efficiency for Cyt *f* oxidation and the rate constants varied greatly (Figure 1 and Table 1). As can be inferred from the kinetic profiles in Figure 1, R93E Pc is drastically impaired in oxidizing Cyt *f*. Figure 1 also shows the kinetic trace for the L14A mutant, which is also less reactive than WT Pc but presents the highest extent of Cyt *f* oxidation, a fact that can be ascribed to its more positive redox potential (Table 1). The k_{obs} values for the reduction of most mutants by Cyt *f* are independent of Pc concentration (Figure 2, top), as was the case for WT Pc, just allowing the determination of the apparent k'_{et} for the reaction. The exceptions are mutants K35E and R93E, which present a nonlinear dependence of k_{obs} on Pc concentration (Figure 2, bottom). Applying the formalism in ref *11*, we can estimate the minimal values for k'_{et} and K_A. However, the lack of points at low Pc concentrations only makes the k'_{et} values reliable, although the profiles in Figure 2 clearly indicate that the Cyt *f*−Pc association is drastically impaired in these two mutants. Table 1 shows that most mutants yield k'_{et} values smaller than that of WT Pc, with the exception of the D54K mutant, which exhibits a higher reactivity, and the two Tyr-88 mutants, which behave like

WT Pc, thus indicating that this residue is not involved in the interaction of Pc with Cyt *f*.

These data are also in agreement with the paramagnetic NMR structural analysis of the *Nostoc* Cyt *f*−Pc complex recently performed by Díaz-Moreno et al. (Figure 4, and see ref *14*), who reported that the binding interface involves the hydrophobic areas close to the metal centers in both proteins. In Pc, in particular, it comprises 14 residues, namely, 10 from the hydrophobic patch (Leu-14, Val-36, Pro-37, Pro-38, Leu-64, Met-66, Pro-68, Pro-91, His-92, and Ala-95), three from the adjacent region of site 2 (Lys-62, Gln-63, and Glu-90), and the neighboring Lys-35. A second, minor recognition site on Pc corresponds to residues Asp-54 and Lys-57, which are both electrostatically interacting with charged residues of Cyt *f* (*14*).

As expected, all mutants at the hydrophobic patch exhibited a significant decrease in their reactivity (Table 1), as did all of them when interacting with PSI (*27*). It is important to consider that only a qualitative comparison of the effect of mutations on both systems can be made, due to the different nature of the corresponding kinetic constants. On the other hand, point charge mutations for decreasing the positive charge of the east patch weakened the ability of Pc to oxidize Cyt *f*, whereas mutations to make the copper protein more positive enhanced the redox interaction rate. A similar behavior was observed for the interaction of all these mutants with PSI (*27*). The more drastic effect was observed with the R93E mutant, in which the mutation induced a severe decrease in the rate of electron transfer both from Cyt *f* and to PSI (Table 1), thus revealing the crucial role that such a residue—which is the only arginine in the primary structure of cyanobacterial Pc—plays in the interaction of Pc with its two redox partners.

The effect of ionic strength on the interaction of Pc mutants with Cyt *f* was also analyzed with the aim of investigating the effect of mutations on the electrostatic nature of the interaction. Most mutants present an ionic strength dependence profile similar to that of WT (Figure 3), thus indicating that attractive electrostatic interactions are stabilizing the complex; the more pronounced the profile of the decrease of k_{obs} with ionic strength, the stronger the Cyt *f*−Pc electrostatic interaction. The only exception is the R93E mutant, for which the k_{obs} values are independent of ionic strength, as also occurred in its interaction with PSI (*27*). The surface electrostatic potential distribution previously calculated for WT Pc and mutants D54K and R93E (*27*) showed that the mutation at position 54 considerably spreads the positive surface electrostatic potential, whereas the replacement at position 93 makes the positive area almost disappear. In the Cyt *f*−Pc interaction in *Phormidium*, it has also been shown that removing negative charges in Pc increased the dependence on ionic strength, whereas removing positive charges decreased it. Moreover, mutations offsetting or inverting the electrostatic charge in position R93 converted electrostatic attraction into repulsion (*13*). Similarly, as a general rule, in *Nostoc* the ionic strength dependence of the rate constant can be related to the intensity of the positive patch in Pc. It is worth noting that residues Lys-62, Arg-93, and Lys-35 in Pc seem to be involved in Cyt *f*−Pc complex formation, in agreement with the structure of the complex recently determined (ref *14* and Figure 4).

CONCLUDING REMARKS

This work provides novel insights into the peculiar structural features of the *Nostoc* Cyt *f*−Pc complex, revealing the very different relevance of the role played by Pc residues involved in the bimolecular interaction.

Moreover, the parallel kinetic behavior of Pc mutants when reacting with both Cyt *f* and PSI clearly demonstrates that the copper protein uses the same surface areas to interact with its two redox partners, one electrostatic for driving the attractive movement and complex formation and the other hydrophobic for electron transfer.

ACKNOWLEDGMENT

REFERENCES

1. Hope, A. B. (2000) Electron transfer amongst cytochrome *f*, plastocyanin and photosystem I: Kinetics and mechanisms, *Biochim. Biophys. Acta 1456*, 5−26.
2. Hervás, M., Navarro, J. A., and De La Rosa, M. A. (2003) Electron transfer between soluble proteins and membrane complexes in photosynthesis, *Acc. Chem. Res. 36*, 798−805.
3. Gray, J. C. (1992) Cytochrome *f*: Structure, function and biosynthesis, *Photosynth. Res. 34*, 359−374.
4. Cramer, W. A., Soriano, G. M., Ponomarev, M., Huang, D., Zhang, H., Martinez, S. E., and Smith, J. L. (1996) Some new structural aspects and old controversies concerning the cytochrome *b₆f* complex of oxygenic photosynthesis, *Annu. Rev. Plant Physiol. Plant Mol. Biol. 47*, 477−508.
5. Kurisu, G., Zhang, H. M., Smith, J. L., and Cramer, W. A. (2003) Structure of the cytochrome *b₆f* complex of oxygenic photosynthesis: Tuning the cavity, *Science 302*, 1009−1014.
6. Martinez, S. E., Huang, D., Szczepaniak, A., Cramer, W. A., and Smith, J. L. (1994) Crystal structure of chloroplast cytochrome *f* reveals a novel cytochrome fold and unexpected heme ligation, *Structure 2*, 95−105.
7. Chi, Y. I., Huang, L. S., Zhang, Z. L., Fernandez-Velasco, J. G., and Berry, E. A. (2000) X-ray structure of a truncated form of cytochrome *f* from *Chlamydomonas reinhardtii*, *Biochemistry 39*, 7689−7701.
8. Crowley, P. B., Otting, G., Schlarb-Ridley, B. G., Canters, G. W., and Ubbink, M. (2001) Hydrophobic interactions in a cyanobacterial plastocyanin-cytochrome *f* complex, *J. Am. Chem. Soc. 123*, 10444−10453.
9. Crowley, P. B., and Ubbink, M. (2003) Close encounters of the transient kind: Protein interactions in the photosynthetic redox chain investigated by NMR spectroscopy, *Acc. Chem. Res. 36*, 723−730.
10. Hart, S. E., Schlarb-Ridley, B. G., Delon, C., Bendall, D. S., and Howe, C. J. (2003) Role of charges on cytochrome *f* from the cyanobacterium *Phormidium laminosum* in its interaction with plastocyanin, *Biochemistry 42*, 4829−4836.
11. Meyer, T. E., Zhao, Z. G., Cusanovich, M. A., and Tollin, G. (1993) Transient kinetics of electron transfer from a variety of *c*-type cytochromes to plastocyanin, *Biochemistry 32*, 4552−4559.
12. Wagner, M. J., Packer, J. C., Howe, C. J., and Bendall, D. S. (1996) Some characteristics of cytochrome *f* in the cyanobacterium *Phormidium laminosum*: Its sequence and charge properties in the reaction with plastocyanin, *Biochim. Biophys. Acta 1276*, 246−252.
13. Schlarb-Ridley, B. G., Bendall, D. S., and Howe, C. J. (2002) Role of electrostatics in the interaction between cytochrome *f* and plastocyanin of the cyanobacterium *Phormidium laminosum*, *Biochemistry 41*, 3279−3285.
14. Díaz-Moreno, I., Díaz-Quintana, A., De la Rosa, M. A., and Ubbink, M. (2005) Structure of the complex between plastocyanin and cytochrome *f* from the cyanobacterium *Nostoc sp.* PCC 7119 as determined by paramagnetic NMR, *J. Biol. Chem. 280*, 18908−18915.

15. Díaz-Quintana, A., Navarro, J. A., Hervás, M., Molina-Heredia, F. P., De la Cerda, B., and De la Rosa, M. A. (2003) A comparative structural and functional analysis of cyanobacterial plastocyanin and cytochrome *c₆* as alternative electron donors to photosystem I, *Photosynth. Res. 75*, 97−110.
16. Kaneko, T., Nakamura, Y., Wolk, C. P., Kuritz, T., Sasamoto, S., Watanabe, A., Iriguchi, M., Ishikawa, A., Kawashima, K., Kimura, T., Kishida, Y., Kohara, M., Matsumoto, M., Matsuno, A., Muraki, A., Nakazaki, N., Shimpo, S., Sugimoto, M., Takazawa, M., Yamada, M., Yasuda, M., and Tabata, S. (2001) Complete genomic sequence of the filamentous nitrogen-fixing cyanobacterium *Anabaena* sp. strain PCC 7120, *DNA Res. 8*, 205−213.
17. Molina-Heredia, F. P., Balme, A., Hervás, M., Navarro, J. A., and De la Rosa, M. A. (2002) A comparative structural and functional analysis of cytochrome *cₘ*, cytochrome *c₆* and plastocyanin from the cyanobacterium *Synechocystis* sp. PCC 6803, *FEBS Lett. 517*, 50−54.
18. Erdeniz, N., Mortensen, U. H., and Rothstein, R. (1997) Cloning-free PCR-based allele replacement methods, *Genome Res. 7*, 1174−1183.
19. Molina-Heredia, F. P., Hervás, M., Navarro, J. A., and De la Rosa, M. A. (1998) Cloning and correct expression in *E. coli* of the petE and petJ genes respectively encoding plastocyanin and cytochrome *c₆* from the cyanobacterium *Anabaena* sp. PCC 7119, *Biochem. Biophys. Res. Commun. 243*, 302−306.
20. Rippka, R., Deruelles, J., Waterbury, J. B., Herdman, M., and Stanier, R. Y. (1979) Generic assignments, strain histories and properties of pure cultures of cyanobacteria, *J. Gen. Microbiol. 111*, 1−61.
21. Bendall, D. S., Davenport, H. E., and Hill, R. (1971) Cytochrome components in chloroplasts of the higher plants, *Methods Enzymol. 23*, 327−344.
22. Bendall, D. S., Bowes, A. C., Stewart, A. C., and Taylor, M. E. (1988) Oxygen-evolving Photosystem-II particles from *Phormidium laminosum*, *Methods Enzymol. 167*, 272−280.
23. Ubbink, M., Ejdeback, M., Karlsson, B. G., and Bendall, D. S. (1998) The structure of the complex of plastocyanin and cytochrome *f*, determined by paramagnetic NMR and restrained rigid-body molecular dynamics, *Structure 6*, 323−335.
24. Arslan, E., Schulz, H., Zufferey, R., Kunzler, P., and Thony-Meyer, L. (1998) Overproduction of the *Bradyrhizobium japonicum c*-type cytochrome subunits of the cbb₃ oxidase in *Escherichia coli*, *Biochem. Biophys. Res. Commun. 251*, 744−747.
25. Sambrook, J., Fritsch, E. F., and Maniatis, T. (1989) *Molecular Cloning: A Laboratory Manual*, 2nd ed., Cold Spring Harbor Laboratory Press, Plainview, NY.
26. Eftekhar, F., and Schiller, N. L. (1994) Partial purification and characterization of a mannuronan-specific alginate lyase from *Pseudomonas aeruginosa*, *Curr. Microbiol. 29*, 37−42.
27. Molina-Heredia, F. P., Hervás, M., Navarro, J. A., and De la Rosa, M. A. (2001) A single arginyl residue in plastocyanin and in cytochrome *c₆* from the cyanobacterium *Anabaena* sp. PCC 7119 is required for efficient reduction of photosystem I, *J. Biol. Chem. 276*, 601−605.
28. Appleby, C. A. (1969) Electron transport systems of *Rhizobium japonicum*. II. *Rhizobium* haemoglobin, cytochromes and oxidases in free-living (cultured) cells, *Biochim. Biophys. Acta 172*, 88−105.
29. Navarro, J. A., Hervás, M., De la Cerda, B., and De la Rosa, M. A. (1995) Purification and physicochemical properties of the low-potential cytochrome *c₅₄₉* from the cyanobacterium *Synechocystis* 6803, *Arch. Biochem. Biophys. 318*, 46−52.
30. Navarro, J. A., Hervás, M., Pueyo, J. J., Medina, M., Gómez-Moreno, C., De la Rosa, M. A., and Tollin, G. (1994) Laser flash-induced photoreduction of photosynthetic ferredoxins and flavodoxin by 5-deazariboflavin and by a viologen analogue, *Photochem. Photobiol. 60*, 231−236.
31. Hervás, M., Navarro, J. A., Díaz, A., Bottin, H., and De la Rosa, M. A. (1995) Laser-flash kinetic analysis of the fast electron transfer from plastocyanin and cytochrome *c₆* to photosystem I. Experimental evidence on the evolution of the reaction mechanism, *Biochemistry 34*, 11321−11326.
32. Molina-Heredia, F. P., Wastl, J., Navarro, J. A., Bendall, D. S., Hervás, M., Howe, C. J., and De La Rosa, M. A. (2003) Photosynthesis: A new function for an old cytochrome? *Nature 424*, 33−34.
33. Ponamarev, M. V., Schlarb, B. G., Howe, C. J., Carrell, C. J., Smith, J. L., Bendall, D. S., and Cramer, W. A. (2000) Tryp-

tophan-heme π-electrostatic interactions in cytochrome *f* of oxygenic photosynthesis, *Biochemistry 39*, 5971−5976.

34. Tollin, G. (1995) Use of flavin photochemistry to probe intraprotein and interprotein electron-transfer mechanisms, *J. Bioenerg. Biomembr. 27*, 303−309.

35. Navarro, J. A., Cheddar, G., and Tollin, G. (1989) Laser Flash Photolysis studies of the kinetics of reduction of spinach and *Clostridium* ferredoxins by a viologen analogue: Electrostatically controlled nonproductive complex formation and differential reactivity among the iron−sulfur clusters, *Biochemistry 28*, 6057−6065.

36. Qin, L., and Kostic, N. M. (1992) Electron-transfer reactions of cytochrome *f* with flavin semiquinones and with plastocyanin. Importance of protein−protein electrostatic interactions and donor−acceptor coupling, *Biochemistry 31*, 5145−5150.

37. Watkins, J. A., Cusanovich, M. A., Meyer, T. E., and Tollin, G. (1994) A "parallel plate" electrostatic model of bimolecular rate constants applied to electron-transfer proteins, *Protein Sci. 3*, 2104−2114.